Recibido: 04/04/2024
Aceptado: 15/07/2024

REVISTA DE TELEDETECCIÓN
Asociación Española de Teledetección
(2024) 64, 1-14
ISSN 1133-0953
EISSN 1988-8740
https://doi.org/10.4995/raet.2024.21467

Application of the METRIC model to estimate maize crop evapotranspiration at field scale with Google Earth Engine

Victor Manuel Gordillo-Salinas *[1], Juan Arista-Cortes [1], Nora Meraz-Maldonado [2], Waldo Ojeda-Bustamante [3], Raúl Enrique Valle-Gough [4], Sergio Iván Jiménez-Jiménez [1]

[1] *Instituto Mexicano de Tecnología del Agua, Paseo Cuauhnáhuac, 8532 Progreso, Jiutepec C.P. 62550 Morelos, Mexico.*

[2] *Colegio de Postgraduados, carretera México-Texcoco km 36.5, C.P. 56230, Montecillo, Texcoco, Estado de México, México.*

[3] *Colegio Mexicano de Ingenieros en Irrigación (COMEII), Vicente Garrido 106, C.P. 62230, Col. Ampl. Maravillas, Cuernavaca, México.*

[4] *Universidad Autónoma de Baja California, Instituto de Ciencias Agrícolas, Carretera Delta S/N, C.P. 21705, Ejido Nuevo León, Mexicali, Baja California, México.*

[5] *INIFAP-CENID RASPA Centro Nacional de Investigación Disciplinaria en Relación Agua-Suelo-Planta-Atmósfera. Margen Derecha Canal Sacramento km 6.5, Zona Industrial, C.P. 35140, Gómez Palacio, Durango, México.*

Abstract: Determination of actual crop evapotranspiration (ETc) is a crucial challenge for sustainable irrigation water management. In this sense, robust and accurate estimation models of crop water consumption along with spatial tools and processing platforms in the cloud are necessary to determine the timing and amount of irrigation needed as a first step toward proposing solutions and water use efficiency. The objective of this study was to determine maize crop evapotranspiration using the algorithms of the Mapping Evapotranspiration at High Resolution with Internalized Calibration (METRIC) model in the Google Earth Engine (GEE) platform. The crop was monitored with 14 Landsat images during its growth period. ETc values with METRIC were compared with ETc obtained with the FAO-56 methodology, and the cumulative ETc was compared with ETc derived from a soil moisture sensor. The evaluation between the METRIC model and FAO-56 displayed a determination coefficient (R^2) of 0.87, mean squared error (MSE) of 0.8 mm/day, and bias percentage (PBIAS) of -14.5. According to the cumulative ETc, the difference was 16 mm for METRIC and 63 mm for FAO-56, compared with moisture sensor values. METRIC overestimated by 3.0% (PBIAS=-3.0), and FAO-56 underestimated by 11.9% (PBIAS=11.9). The results and the programmed algorithms in this work can be the basis for future calibrations and validations of the evapotranspiration of different crops.

Key words: evapotranspiration; Google Earth Engine, FAO-56, energy balance, soil moisture.

Aplicación del modelo METRIC para estimar la evapotranspiración del cultivo de maíz a escala de campo en Google Earth Engine

Resumen: La determinación de la evapotranspiración de cultivos es el principal desafío para el manejo sustentable del agua para riego. En este sentido, se requieren modelos robustos y precisos para determinar el consumo de agua que junto con herramientas de análisis espacial y plataformas de procesamiento en la nube permiten establecer el momento y cantidad de riego requerido, como un primer paso para proponer soluciones para el ahorro y uso eficiente de agua demandada por los cultivos para satisfacer sus requerimientos hídricos. El objetivo de este estudio fue determinar la evapotranspiración del cultivo de maíz (ETc) utilizando el algoritmo de Mapeo de evapotranspiración con calibración internalizada en alta resolución (METRIC) y la plataforma de Google Earth

To cite this article: Gordillo-Salinas, V. M., Arista-Cortes, J., Meraz-Maldonado, N., Ojeda-Bustamante, W., Valle-Gough, R. E., Jiménez-Jiménez, S. I. 2024. Application of the METRIC model to estimate maize crop evapotranspiration at field scale with Google Earth Engine. *Revista de Teledetección*, *64*, 1-14. https://doi.org/10.4995/raet.2024.21467

* *Corresponding author: manuel_gordillo@tlaloc.imta.mx*

Engine (GEE). El cultivo fue monitoreado con 14 imágenes Landsat (Landsat 8 y 9). Los valores de ETc obtenidos con METRIC fueron comparadas con los obtenidos con el modelo de FAO-56 y la lámina de agua acumulada en el suelo medida con un sensor de humedad. La evaluación entre los modelos de METRIC y FAO-56 mostraron un coeficiente (R^2) DE 0,87, un error cuadrado promedio (MSE) de 0.8 mm/día y un porcentaje de sesgo (PBIAS) de -14,5. De acuerdo con el consumo total de agua registrada por el sensor de humedad, la diferencia entre METRIC y FAO-56 fue de 16 mm y 63 mm respectivamente. Se observó que METRIC sobreestima un 3,2% (PBIAS=-3,0) y FAO-56 subestima un 11,9% (PBIAS=11,9). Los resultados y el algoritmo programado en este trabajo pueden ser la base para futuras calibraciones y validaciones de ETc para distintos cultivos.

Palabras clave: evapotranspiración, Google Earth Engine, FAO-56, balance de energía, humedad del suelo.

1. Introducción

Optimizing water use in irrigated agriculture plays an important role in the face of the economic and environmental challenges of guaranteeing the profitability of agriculture and the sustainability of water resources. This requires the estimation of water use and efficiency indicators (e.g. crop evapotranspiration) to identify system inefficiencies as a first step towards proposing solutions.

The most common method to estimate crop water requirements and crop evapotranspiration is the FAO 56 described in Allen *et al.*, (1998). Despite the significant progress that has been achieved with the FAO 56 method, the main limitations include the possibility of spatial estimates of evapotranspiration (ET), and therefore, the lack of understanding of the fine-scale spatial variation in inputs and outputs.

Other methods to estimate and measure ET include lysimeters, Eddy covariance, Bowen ratio, humidity balance, sap flow, scintillometry and remote sensing (Allen *et al.*, 2011). In this sense, the use of remote-sensing (RS) based models are a feasible alternative to determine the crop water requirements, since they help monitoring large irrigation surfaces (Suwanlertcharoen *et al.*, 2023).

RS models may be separated into two main groups: models based on vegetation indices (VI) and the models based on the temperature of the surface (Ts). The VI models are based on the vegetation greenness indices, such as the Normalized Difference Vegetation Index (NDVI; Rouse *et al.*, 1973) and weather data, mainly net radiation (Rn), vapor pressure deficit (VPD) and air temperature (Ta) (Laipelt *et al.*, 2021). While the procedures to estimate ET via Ts, such as remote sensing-based energy balance (RSEB) models, which estimate actual evapotranspiration (ETa) values for each pixel via a surface energy balance by taking into account of total available energy at the surface and the amount heat fluxes (conducted into soil and convected into the air above the surface) (Kilic *et al.* 2016).

All models of energy balance have assumptions, advantages and disadvantages; for example, SEBAL (Surface Energy Balance Algorithm for Land) model (Bastiaanssen *et al.* 1998) considers a lineal relation between land surface temperature and temperature difference for distinct height and stablishes ET=0 for dry pixel, however it requires fewer ground data and atmospheric correction is not much needed, but it only can be used on plain terrain and the anchor pixel depends on users selection.

On another hand, METRIC model relates land surface temperature and temperature difference for distinct height, considering constant the reference ET Fraction throughout the day and stablishing ET=0 for hot pixel, however it requires fewer ground data and can be used for terrain with more rugged topography but presents uncertainty to the choice of the anchor pixel (Aryalekshmi *et al.*, 2021).

A key advantage between SEBAL and METRIC models is the estimation of the temperature gradient (dT) between a height z1 and z2, which overcomes the difficulty of accurately estimating surface temperature from satellites (Allen *et al.*, 2011).

The dT is estimated, in both models, by selecting two extreme conditions known as cold pixels

and hot pixels, however, the models differ in the selection of the cold pixel; while in SEBAL a pixel belonging to a water body is selected assuming that H is zero, METRIC recommends a cold pixel belonging to an agricultural field with full cover and no water limitation in the soil assuming that ET rates are 5% higher than the reference evapotranspiration of alfalfa (Allen *et al*., 2007).

METRIC model estimates the crop water requirements using the residual energy balance equation on surface (Allen *et al.*, 2007). This model has displayed an adequate performance for water consumption estimation in different crops worldwide and it has been validated with results obtained with distinct measurement instruments such as lysimeters, eddy covariance towers and atmometers (Pôças *et al.*, 2014; French *et al.*, 2015; Reyes-González *et al.*, 2017; Khan *et al.*, 2019; Lima *et al.*, 2020).

Processing ET models using remote sensing requires cloud platforms with high-performance computing that provide collections of satellite images and land climate databases, which can be used to monitor agricultural fields at different temporal and spatial scales (Laipelt *et al.*, 2021).

In this way, there are ET free access platforms, for example, SEBAL open source python script or Py-SEBAL (https://github.com/wateraccounting/SEBAL), FAO Water Productivity Open-access portal (WaPOR; https://wapor.apps.fao.org/home/WAPOR_2/1), Earth Engine Evapotranspiration Flux (EEFLUX; Allen *et al.*, 2015) and METRIC-Gis toolbox (Ramírez-Cuesta *et al.,* 2020).

Other products available for getting evapotranspiration are MOD16 and LSA-SAF MSG ET, both available with 1 km and 5 km of spatial resolution, respectively, for global scales (Jahangir and Arast, 2020)

There is a version of METRIC that runs on Google Earth Engine (GEE) platform (http://eeflux-level1.appspot.com/). However, users cannot alter or amend the available code and only to select the site of interest is allowed (Mhawej and Faour, 2020).

Due to its automated nature and its dependence on cloud data, the ET estimation model platforms have the potential to evaluate water use and improve irrigation water management in large extensions with extremely low cost (Kadam *et al.*, 2021).

In Northwest of Mexico predominates dry climate and the irrigation water volume available in this zone is limited by rainwater captured by the dams and it determines total the irrigations and the list of crops authorized per agricultural cycle (Ramírez-Sánchez *et al.,* 2021). In this sense, the implementation of remote sensing to estimate crop evapotranspiration can help water management in Mexico, however, this depends on solid measurements.

Due the high performance of METRIC model and the importance of maize crop in the study area, the aims of this research were (1) to calculate ETc using the METRIC model in Google Earth Engine (GEE) with Landsat images for a maize plot; (2) to compare daily ETc values obtained with METRIC and FAO-56 methodology; and (3) to compare the accumulated ETc in the crop growth period among the METRIC model, FAO-56 methodology, and the measurements recorded in a soil moisture sensor installed in the field.

2. Materials and Methods

2.1. Study area

The study was carried out in an experimental field (0.1 ha) of the Produce Sinaloa Foundation (107° 30’ 15.847’’W, 24° 47´19.295´´N, 60 m above sea level), located in one of the most important Mexican large-scale irrigated areas in the northwest region of Mexico (Figure 1).

The weather of the region is semiarid, with annual average rainfall of 690 mm. The rainy season starts in July and finishes in September (with around 79% of the annual rainfall), and the driest season is from February to May (with only 1.3% of the annual rainfall). The monthly average Ta varies from 19.2 °C in January to 30 °C in July (Avendaño-López *et al.*, 2015).

Maize grain is the most commonly irrigated crop in the study area with a surface about of 120 000 ha and a crop yield of 13 t/ha (Conagua, 2023). A maize experimental field was set up with a density of 100 000 plants/ha. The sowing date was on November 15th, 2021, and harvest date was on May 12th, 2022 (178-day crop cycle). The soil of the experimental area had a

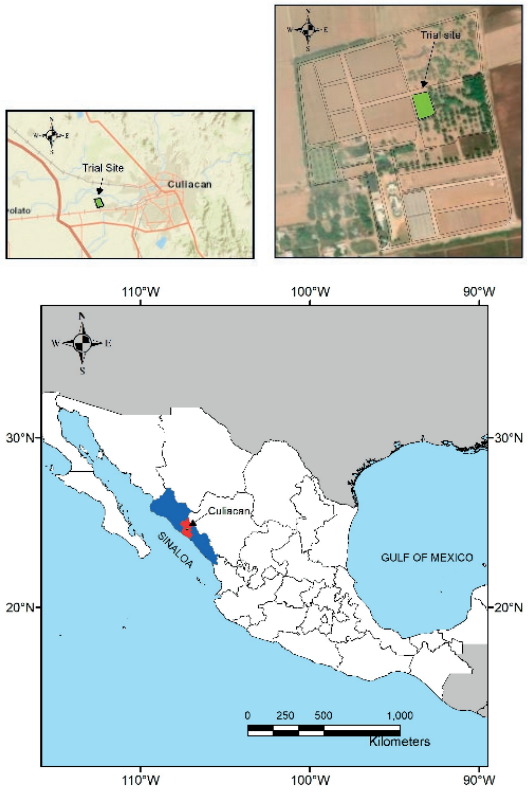

Figure 1. Study area. Field: Foundation Produce Sinaloa, México.

silt-loam texture (19.08% Sand, 60% Silt, and 20.92% Clay) and a bulk density of 1.27 g/cm^3. Field capacity (FC) and permanent wilting point (PWP) were determined in the laboratory (Table 1, QuimiaLab, Los Mochis, Sinaloa, Mexico). The soil volumetric moisture content was 34.29% and 20.32% at FC and PWP, respectively.

Table 1. Physical-chemical characteristics of the soil for the area of study.

variable	Result	Unit	Interpretation
pH 1:2	7.46	U pH	Moderately alkaline
C.E.	1.14	ds/m	Low/Normal
Point of saturation	50	%	Optimum
FC	34.29	%	High
PWP	20.32	%	High
Bulk density	1.27	g/cm^3	

Irrigation management was carried out based on irrigation scheduling using CropWat 8.0 software and applied by a surface irrigation system. Calculations are based on guidelines for calculating crop water requirements (Allen *et al.*, 1998), which consider crop parameters, soil characteristics, and climate data to carry out a daily soil water balance (Licht and Archintoulis, 2017). Five irrigation events were applied. Table 2 summarizes the events of water contribution, the depths consumed, and the depth accumulated during the entire cycle.

2.2. Weather data and soil water measurements

The METRIC model requires weather data to estimate the different surface energy balance components, as well as to determine reference evapotranspiration (ETr). The weather data included Ta (°C), relative humidity (%), rainfall (mm), wind speed (m/s), and solar radiation (W/m^2), and were obtained from an automatic weather station at 10-min time intervals (WatchDog Series 2000, Spectrum Technologies, Inc., Aurora, Illinois, USA).

Figure 2 shows the weather variables of maximum, minimum, and average Ta for the crop growing period. A reduction of this variable is notorious from December 2021 to March 2022, with an extreme minimum Ta of 2.8 °C on March 11th, 2022. Rainfall for December 31st, 2023, was approximately 10 mm.

Soil water measurements were made with the CropX (CropX Ltd., Tel Aviv, Israel) sensor. CropX is an electromagnetic sensor that measures soil volumetric water content (θv) (m^3/m^3) based on the amplitude domain reflectometry (ADR) at 20 and 46 cm depths in the soil. The sensor has a helical central axis design to reduce soil disturbance (Datta *et al.*, 2018). This sensor relies on an electromagnetic signal related to the dielectric permittivity to calculate the soil water content (Zawilski, *et al.*, 2023).

The θv readings were registered *in situ* on a daily way, which determined crop water consumption through a water balance, and subsequently, the measurements were integrated to know the evapotranspiration throughout the crop growing season.

Table 2. Water management in soil during the period of analysis.

Date	Event	DAS (days)	Interval (days)	Consumption (mm)	Accumulated consumption (mm)	Irrigation (mm)
Nov 15, 21	Sowing Irrigation	0	0	0	0	182
Dec 31, 21	Rainfall	46	46	90	90	0
Jan 20, 22	Irrigation 1	66	20	94	185	180
Feb 12, 22	Irrigation 2	89	23	36	222	213
Feb 26, 22	Irrigation 3	103	14	110	332	195
Mar 28, 22	Irrigation 4	133	30	102	434	195
May 1, 22	Senescence	168	35	81	516	0
May 12, 22	Harvest	180	12	12	529	0

* DAS = Days After Sowing.

2.3. Estimation of ETc using the FAO-56 methodology

The ground-measured ET could have large significant errors by itself (up to 29% error for measurements made by eddy covariance). Therefore, validation of satellite-based ET estimation with ground-measured ET shows uncertainties (Tasumi, 2019). For this study there is no ground measured ET, therefore the accuracy of the model was evaluated via comparisons with ET determined using FAO-56 methodology (Equation 1), which was proposed in other works (Stancalie *et al.*, 2010; Tasumi, 2019, Pereira *et al.*, 2015).

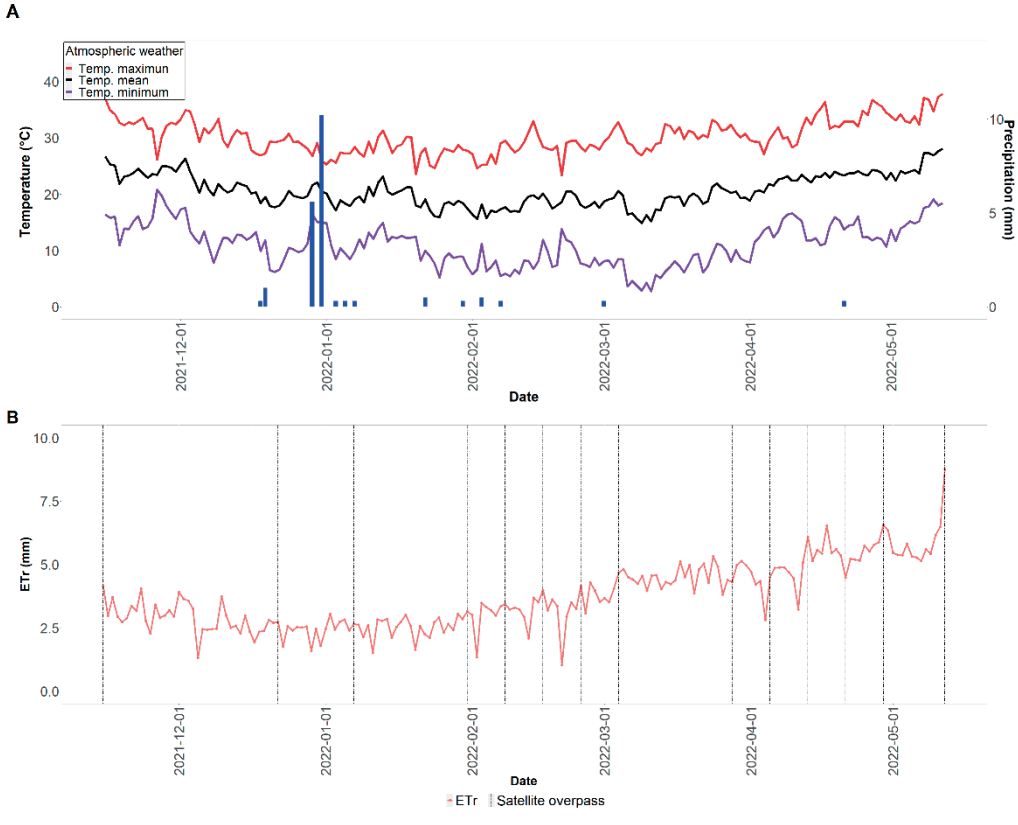

Figure 2. Daily values of air temperature (Ta) and precipitation events (A) and reference evapotranspiration (B) during the crop growing season. The acquisition images dates are shown with vertical dashed lines.

Table 3. Crop coefficient for the maize crop, taken from manual 70 of the ASCE, using alfalfa as a reference crop.

Stage	Duration (days)	Crop coefficient (Kc)
Initial	30	0.2
Development	50	Positive linear relationship between values 0.2 and 1.0
Mean	60	1.0
Final	40	Negative linear relationship between values from 1.0 to 0.18

The FAO-56 methodology for estimating ETc is considered a two-step method in which ETr is determined, and later, based on the crop phenological stage, it is assigned a crop coefficient (Kc). Using Equation 1, the ETc was determined throughout the entire crop cycle.

$$ET_c = K_c \cdot ET_r \quad (1)$$

In this study, ETr (mm) was determined by the ASCE Penman-Monteith Standardized method (ASCE-EWRI, 2005), and Kc (dimensionless) values for maize (Table 3) were taken from tables reported in manual 70 of the American Society of Civil Engineers (ASCE) for each of the crop development stages (Jensen and Allen, 2016).

2.4. METRIC model and remote sensing data

METRIC model is based on satellite image processing to calculate actual evapotranspiration (ETa) as a residual of the surface energy balance, and it is does not require knowledge of the phenological stage or the type of crop, which has an advantage over traditional methods of crop coefficient curves and vegetation indices (Allen *et al.*, 2011). ETa is estimated with Equation 2:

$$LE = R_n - G - H \quad (2)$$

Where LE is latent heat flux (latent energy consumed by ET, W/m^2); the Rn, considered as the net radiation (W/m^2), is the energy available on the surface (balance of all incoming and outgoing short-wave and long-wave radiation at the surface); G is the soil heat flux (W/m^2), and it is considered as the energy needed to heat the soil; and finally, H is the sensible heat flux (W/m^2), and it is the energy used to heat the air. A detailed description of the theoretical bases and principles is presented by Allen *et al.* (2007).

This study implemented the algorithms of the METRIC model with Landsat-8 and Landsat-9 images in Google Earth Engine (GEE) platform with JavaScript. GEE is a cloud-based geospatial analysis platform consisting of a catalogue of several petabytes of satellite images. It can be accessed and controlled via an App Programming Interface (API), accessible via the Internet and an associated web-based Interactive Development Environment (IDE) that helps quickly create prototypes and the visualization of results (Gorelick *et al.*, 2017).

Fourteen clear-sky Landsat images (Path=32/Row=43) covered the maize crop growing season. Landsat satellites obtain images of the entire Earth's surface at a 30-m spatial resolution and 16-day temporal resolution, including multispectral and thermal data. The images Landsat-8 (6 images; source: https://developers.google.com/earth-engine/datasets/catalog/LANDSAT_LC08_C02_T1) and Landsat-9 (8 images; source: https://developers.google.com/earth-engine/datasets/catalog/LANDSAT_LC09_C02_T1) were selected from Earth Engine Data Catalogue, which fulfilled the condition of the presence of cloudiness under 10%, achieving high-quality images.

RSEB models (like METRIC) estimate Rn, G y H using surface reflectance and surface temperature from satellite platforms such as MODIS, Landsat and ASTER (De la Fuente-Sáiz *et al.*, 2017). Allen *et al.* (1998) mentioned four stages growth for the maize crop cycle, under standard conditions and García *et al.* (2013) reported the minimum image requirement to develop the crop coefficient (Kc) for maize. They mentioned that at least one image is required for the crop plantation date, in which one Kc is represented for bare soil, and hence describe the behaviour of the crop in the initial stage. In the development stage, they recommend at least four images, considering this stage critical for the crop, due to the quick change of the biomass. The middle stage considered the period with the highest ETc and stable values at

the same time. As long as irrigation management is adequate, it only requires one image. Finally, the final stage, using at least two images as recommended by García *et al.* (2013), begins with a high Kc value and ends with very low values, assuming a proportional reduction.

This study accomplished the minimum requirements mentioned by García *et al.* (2013). The Landsat 8 satellite presented only one image in the initial stage, none in the development stage, and more in the range comprised by middle and final crop stages. On the other hand, Landsat 9 produced no available images in the initial stage, two in the development stage, and the rest in the middle and final stages.

Kilic *et al.* (2020) mentioned that the implementations of remote sensing-based energy balance models (EEFlux and eeMETRIC) onto GEE have enabled robust automation and producing of accurate and consistent ET maps.

2.5. Statistical analysis

To evaluate the METRIC model implemented in GEE, it was compared with FAO-56 approach. Five statistical indices were used: root mean square error (RMSE), mean bias error (MBE), Percent bias (PBIAS), mean absolute error (MAE), and mean squared error (MSE).

a)RMSE is calculated as:

$$RMSE = \sqrt{\left[\frac{\sum_{i=1}^{n}(O_i - P_i)^2}{n}\right]} \quad (3)$$

b)MBE is calculated as:

$$MBE = \frac{1}{n}\sum_{i=1}^{n}(O_i - P_i) \quad (4)$$

c)PBIAS is calculated as:

$$PBIAS = \left[\frac{\sum_{i=1}^{n}(O_i - P_i)}{\sum_{i=1}^{n} O_i}\right] \times 100 \quad (5)$$

d)MAE is calculated as:

$$MAE = \frac{\sum_{i=1}^{n}|P_i - O_i|}{n} \times 100 \quad (6)$$

e)MSE is calculated as:

$$MSE = \frac{1}{n}\sum_{i=1}(O_i - P_i)^2 \quad (7)$$

Where n is the sample size, Oi is the control value, and Pi is the estimated value.

The accuracy assessment via comparison between FAO-56 with METRIC model was carried out with the same statistical metric mentioned above. In addition, the accumulated ET values obtained with METRIC-GEE and FAO-56 ET were evaluated by comparing the accumulated water depth recorded by Cropx sensor during the growing season to find the existing differences in total water consumption.

3. Results and discussion

3.1. Climatic conditions and ETr

During the study period (from November 2021 to May 2022) dry and hot atmospheric conditions were observed. Maximum values for Ta and ETr were 37.8 °C and 8.8 mm/day, and means of 20.6 °C and 3.7 mm/day, respectively (Figure 2). Cumulative ETr in the study period was 663 mm, and the total precipitation was 20 mm with a maximum value observed on December 31, 2021 (10 mm).

3.2. Calculation of ET with the METRIC model in GEE

The images were processed in the GEE platform to determine the energy balance components (Rn, G, H and LE), as well as the reference ET Fraction (ETrF) and the daily ETc. Table 4 shows the results of the algorithm processing for each day of the scenes.

Rn showed a value range from 400 to 650 W/m^2, with maximum values in the final stage of the crop-growing season (April and May 2022). The maximum amount of energy consumption by G occurred at the beginning and end of the crop cycle. The maximum values of H occurred when the amount of available energy on the surface increases (>Rn) and the demand for energy used by LE decreases. LE used less energy in early and final crop stages, and the maximum value was 510 W/m^2. ETrF showed a maximum value close to 1, which coincides with the values recommended in ASCE manual 70 (Jensen and Allen, 2016). The METRIC model estimated maximum values of ETa about 6 mm/day.

Table 4. Results of the processing of the METRIC energy balance model.

ID	Date	DAS	Rn (W/m^2)	G (W/m^2)	H (W/m^2)	LE (W/m^2)	ETrF (Kc)	ETc (mm/day)	Satellite
1	Nov 12, 21	-3	419	101	91	226	0.52	2.3	L8
2	Dec 22, 21,	38	398	57	22	318	0.97	3.6	L9
3	Jan 07, 22	54	403	37	19	346	1.03	3.8	L9
4	Jan 31, 22	78	442	32	88	320	0.91	4.1	L8
5	Feb 08, 22	86	462	36	111	314	0.96	4.8	L9
6	Feb 16, 22	94	479	38	-69	510	1.04	5.3	L8
7	Feb 24, 22	102	513	44	-5	474	0.99	5.2	L9
8	Mar 04, 22	110	537	47	52	437	0.91	5.4	L8
9	Mar 28, 22	134	602	72	133	396	0.76	4.4	L9
10	Apr 05, 22	142	604	75	255	272	0.83	4.4	L8
11	Apr 13, 22	150	626	90	173	362	0.78	5.8	L9
12	Apr 21, 22	158	638	99	276	261	0.67	3.7	L8
13	Apr 29, 22	166	655	136	239	278	0.64	5.1	L9
14	May 15, 22	182	642	130	432	79	0.20	1.4	L9

* DAS = Days After Sowing.

Several studies have evaluated the performance and accuracy of the components of the energy balance of the METRIC model via comparison between measured and estimated values for LE, Rn, H and G at the satellite overpass date (De la Fuente-Sáiz *et al.*, 2017; Gaso *et al.*, 2017; Ortega-Farias *et al.*, 2016; Ortega-Salazar *et al.*, 2021; Volk *et al.*, 2024; Liu *et al.*, 2024).

Ortega-Farias *et al.* (2016) indicated that the METRIC model underestimated values of Rn by about 5.0 % (RMSE=38 W/m^2), while Gaso *et al.* (2017) reported a relative RMSE of 12% (RMSE=63 W/m^2). Ortega-Salazar *et al.* (2021) and Liu *et al.* (2024) showed that the estimated G with METRIC were overestimated with a RMSE of 40 and 39 W/m^2, respectively. Results showed by De la Fuente-Sáiz *et al.* (2017) found that METRIC underestimated H by about 29% (RMSE=80 W/m^2). However, when using the calibrated functions for aerodynamic roughness length (Zom), METRIC overestimated H by about 5% (RMSE=33 W/m^2). In addition, H was the component of energy balance that showed the major scattering for 1:1 line with a RMSE=92 W/m^2 and relative RMSE=70% for soybean and maize in irrigated and rainfed in Ameriflux sites in Nebraska, USA (Gaso *et al.* 2017).

The Eddy Covariance (EC) technique is the best method for continuous measurement of energy and heat flux (Baldocchi *et al.*, 2001; Baldocchi, 2014); however, several researchers have indicated that turbulent fluxes using the EC technique were less than available energy, which causes a poor closure of energy balance. This EC imbalance can be associated to errors in the measurements of actual ET and therefore to the problems of overestimation of ET by METRIC (Ortega-Farias *et al.*, 2016; Gaso *et al.*, 2017; Ortega-Salazar *et al.* 2021, Tasumi, 2019).

ETrF was obtained for the satellite acquisition dates, being necessary to use a fitting model to estimate the remaining days. The model of a 2nd-degree polynomial fitting reached a high determination coefficient (R^2) of 0.89 for Landsat 8 and Landsat 9 images (Figure 3).

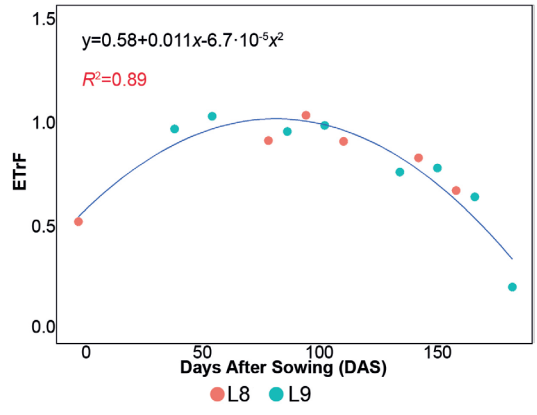

Figure 3. Model for the fitting of the combined ETrF data from satellites Landsat 8 and 9.

This study mixed the ETrF values from Landsat 8 and Landsat 9 to overcome the low temporal

resolution (16 days) and the even distribution of the images acquired by these satellites.

The processing of images in GEE generated different intermediate maps such as Top Of Atmosphere (TOA) reflectance, radiance, albedo, vegetation indices (NDVI, SAVI and LAI), Ts, G, H, LE flux, and others.

Figure 4 shows an example of the deliverables via GEE platform with ETa values for each pixel on two different monitoring dates.

The resulting maps helped to understand the spatial variability of the crop and its characteristics, as well as its behaviour in time. The understanding in time and space will help the farmers, technicians, researchers and others involved to make optimal decisions in the management of agricultural irrigation. In addition, Figure 4 shows a low spatial resolution of the Landsat satellite to analyze the heterogeneity of the study area, which shows the fact that no "pure" pixels fall into the study area, so they contained information for the surrounding areas.

The different elements present in crop fields (plants, trees, soil bare, roads, among others) contribute with the signal captured by sensors and therefore with the mass and energy exchange. The pixels which receive signal from distinct elements are called "mixed" and affect results of models because increase uncertainty drastically during evapotranspiration calculus. However, it is possible to improve results using products with more spatial resolution, and then, for estimating evapotranspiration; the models should account for the presence of a variety of vegetation roughness (Burchard-Levine *et al.* 2021).

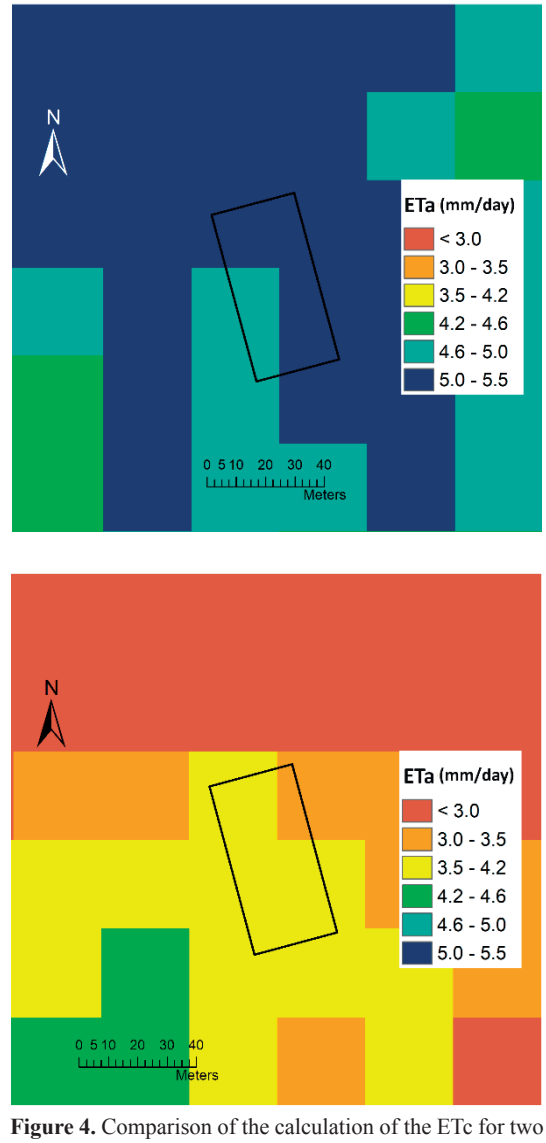

Figure 4. Comparison of the calculation of the ETc for two different dates in the crop growth season. a) ETc on Julian day 47 (February 16th, 2022, 94 DAS), date of monitoring that represents the middle stage of the crop. b) ETc on Julian day 111 (April 21st, 2022, 158 DAS), date of monitoring that represents the final stage of the crop.

3.3. Comparison of the METRIC model and the FAO-56 method

The two ETc estimation methods had a similar temporal trend. Low ETc rates were observed in the initial and final crop growth stages due to null or scarce vegetation and leaf senescence, respectively. Likewise, high ETc rates were observed in the middle stage due to maximum or near maximum plant development (Figure 5). The same pattern was reported in earlier investigations (Pôças *et al.*, 2014; Reyes-González *et al.*, 2017; Tasumi, 2019; Reyes-González *et al.*, 2019). Likewise, FAO-56 was observed to display higher values for ETc, near to 6 mm/day.

An overestimation of the METRIC model was found regarding FAO-56 in the initial stages of the crop, unlike reported by Reyes-González *et al.* (2017). These authors reported that in this stage there is an underestimation of the model when comparing it with data derived from an atmometer and they attributed it to a high value of Kc (0.51).

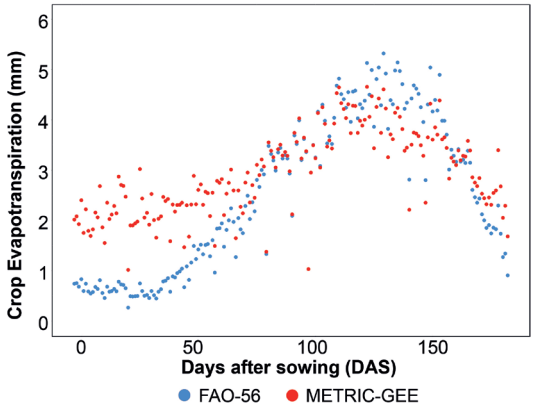

Figure 5. Temporal evolution of the estimated ETc from METRIC and FAO-56 during the entire growing season.

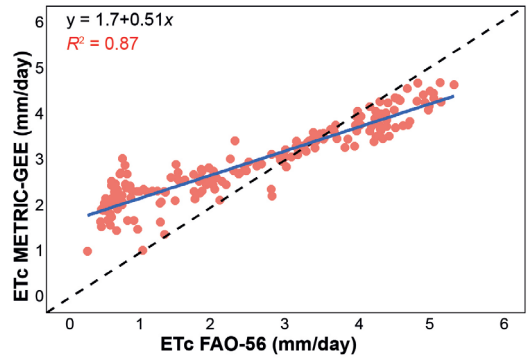

Figure 6. Comparison between FAO-56 and METRIC estimated ETc.

The overestimated values could be due to a heterogeneous surface that influences the surface optical properties (albedo and emissivity), the fraction of absorbed photosynthetically active radiation, the transpiration rate, and surface energy budgets (Guillevic *et al.*, 2012). Sharma *et al.* (2016) evaluated the impact of scale/resolution on evapotranspiration from Landsat and MODIS images and it was observed that Landsat has more preferable spatial resolution (30 m) to map and analyze ETc compared to MODIS (500 m), with regression models explaining 91% and 59% of the variability on BREBS-measured ETc, respectively. Pixel-by-pixel comparisons showed an absolute difference close to 1 mm/day. This difference is mainly due to the underlying assumption of spatial heterogeneity, the difference in spatial, spectral, and radiometric resolution between the Landsat and MODIS sensors.

Figure 6 shows that both methods present a high linear relation with a coefficient of determination (R^2) of 0.87.

Therefore, METRIC can be considered a good predictor of ETc as an alternative to FAO-56, highlighting the advantages of using geospatial tools. The statistical metrics evaluated to determine the accuracy of METRIC model showed a MAE of 0.7 mm/day, MSE of 0.8 mm/day, RMSE of 0.9 mm/day and MBE of -0.4 mm/day.

The PBIAS was -14.5, indicating that METRIC overestimated ETc by 14.5% when compared with the values of the FAO-56 methodology. Model simulation can be considered satisfactory if PBIAS ≤ 15 % (Berreta *et al*., 2014; Feng *et al.*, 2018). Tasumi (2019) evaluated the METRIC model with estimations independent of ETc, using the FAO-56 approach in the Western side of the Urmia Lake basin, in Iran. The MBE for apple, grape, and bare soil were 0.20, 0.16, and 0.36 mm/day, respectively. The positive value of this parameter indicates an overestimation. The MAE were 0.57, 0.52, and 0.59 mm/day and RMSE of 0.73, 0.84, and 0.68 mm/day for the same, respectively.

Reyes-González *et al.* (2017, 2019) carried out evaluation studies for the METRIC model to estimate the ETc for maize in South Dakota, USA. They compared their results with the data from onsite atmometers, and found, for 2017, that R^2=0.87 and RMSE=0.65 mm/day, whereas in 2019, R^2=0.89 and 0.71 mm/day. Overestimations of ETc were found in both experiments.

Finally, Xue *et al.* (2020) evaluated the model for the maize crop in the Central Valley, California, USA, showing an RMSE of 1.2 mm/day with an overestimated relative value of 26% and R^2 of 0.78. The authors concluded that the energy balance models based on remote sensors could be used as support tools for decision-making in precision agriculture to simulate daily ETc and provide information to optimize irrigation management. In general terms, the results presented in this study coincide with reports by different researchers.

3.4. Seasonal evapotranspiration

The seasonal scale in this study referred to accumulated ETc in maize for the whole crop season. Figure 7 shows comparison among FAO-56, METRIC and CropX sensor.

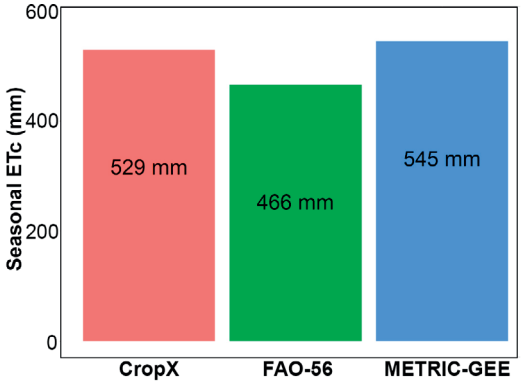

Figure 7. Seasonal ETc (accumulated water depth) estimated using METRIC and FAO-56 models and recorded with the CropX sensor.

When compared to the accumulated ETc measured by the *in situ* sensor, METRIC showed a difference of 16 mm, whereas the FAO-56 methodology showed a difference of 63 mm. The PBIAS of METRIC regarding CropX was -3.0 %, whereas FAO-56 obtained a PBIAS of 11.9%, where negative and positive values mean overestimation and underestimation of the seasonal ETc, respectively.

Results obtained in this study are similar to those reported by Liu *et al.* (2024), where total ETc was 522 mm with METRIC and 533 mm with the soil water balance method. Ojeda-Bustamante *et al*. (2006) determined the maize water consumption in the north of Sinaloa, Mexico, and reported an accumulated consumption of 445 mm. This is lower than obtained in this study, probably due plantation density of 95 000 plants/ha, which is lower than current commercial exploitations densities and different weather conditions for each area of study.

Potential yield is key to predicting the expected crop water use. Lich and Archontoulis (2017) mentioned that higher yields require more water transpiration and, therefore, higher ETc. In general, they claim that to obtain about 10 t/ha of maize, 400 mm of water is required; for 13.5 t/ha, about 510 mm; and for 17 t/ha, about 560 mm.

4. Conclusions

Developing scripts for calculating ETa using a platform as GEE saves processing time and informatics resources due to cloud computer power of google earth engine. Comparing the METRIC model with FAO-56 methodology indicated that METRIC overestimated ETa in early crop stage due to mixed pixels and soil bare probably, so improving spatial resolution is recommended to reduce the error. In the same way, METRIC underestimated in middle stage probably by the anchor pixels selected manually.

Comparing the total ETa obtained among sensors and models showed that soil moisture sensors and METRIC overestimated ETa compared to FAO-56, because the Kc should be adjusted for local conditions probably, so local calibration is recommended for improving comparation.

The model shows a great potential and ability to obtain ET for maize at field scale using satellites and the processing of images on the cloud. Therefore, METRIC could be used in decision-making tools, adding to the development of the precision agriculture field and improving the management of agricultural irrigation.

Acknowledgements

We thank to the directors and technical staff from the Produce Sinaloa foundation, for the support provided during the course of the research.

5. References

Allen, R. G., Pereira, L.S., Raes, D., Smith, M. 1998. Crop evapotranspiration - Guidelines for computing crop water requirements. *FAO Irrigation and drainage paper 56*, Rome.

Allen, R. G., Tasumi, M., Morse, A., Trezza, R., Wright, J. L., Bastiaanssen, W., Kramber, W., Lorite, I., Robison, C. W. 2007. Satellite-Based Energy Balance for Mapping Evapotranspiration with Internalized Calibration (METRIC)—Applications. *Journal of Irrigation and Drainage Engineering*, *133*(4), 395–406. https://doi.org/10.1061/(asce)0733-9437(2007)133:4(395)

Allen, R. G., Pereira, L. S., Howell, T. A., Jensen, M. E. 2011. Evapotranspiration information reporting: I. Factors governing measurement accuracy. *Agricultural Water Management*, *98*(6), 899–920. https://doi.org/10.1016/j.agwat.2010.12.015

Allen, R., Morton, C., Kamble, B., Kilic, A., Huntington, J., Thau, D., Gorelick, N., Erickson, T., Moore, R., Trezza, R., Ratcliffe, I., Robison, C. 2015. EEFlux: A landsat-based evapotranspiration mapping tool on the Google Earth Engine. *Joint ASABE/IA Irrigation Symposium, Emerging Technologies for Sustainable Irrigation*, Long Beach, California https://doi.org/10.13031/irrig.20152143511.

Aryalekshmi, B. N., Biradar, R. C., Chandrasekar, K., Ahamed, J. M. 2021. Analysis of various surface energy balance models for evapotranspiration estimation using satellite data. *The Egyptian Journal of Remote Sensing and Space Science, 24*(3), 1119-1126. https://doi.org/10.1016/j.ejrs.2021.11.007

ASCE–EWRI. 2005. *The ASCE standardized reference evapotranspiration equation*. ASCE–EWRI Standardization of Reference Evapotranspiration Task Committe Rep., ASCE Reston, Va.

Avendaño-López, J. E., Díaz-Valdés, T., Watts-Thorp, C., Rodríguez, J. C., Castellanos-Villegas, A. E., Partida-Ruvalcaba, L., Velázquez-Alcaraz, T. D. J. 2015. Evapotranspiración y coeficientes de cultivo de Chile Bell en el Valle de Culiacán, México. *Terra Latinoamericana, 33*(3), 209–219. http://www.scielo.org.mx/scielo.php?script=sci_arttext&pid=S0187-57792015000300209&lng=es&tlng=es.

Bastiaanssen, W. G. M., Menenti, M., Feddes, R. A., Holtslag, A. A. M. 1998. A remote sensing surface energy balance algorithm for land (SEBAL). *Journal of Hydrology*, *212-213*, 198–212. https://doi.org/10.1016/S0022-1694(98)00253-4

Baldocchi, D. 2014. Measuring fluxes of trace gases and energy between ecosystems and the atmosphere—the state and future of the eddy covariance method. *Global Change Biolology, 20*, 3600–3609. https://doi.org/10.1111/gcb.12649

Baldocchi, D., Falge, E., Gu, L., Olson, R., Hollinger, D., Running, S., ... & Wofsy, S. 2001. FLUXNET: a new tool to study the temporal and spatial variability of ecosystem-scale carbon dioxide, water vapor, and energy flux densities. *Bulletin of the American Meteorological Society, 82*, 2415–2434. https://doi.org/10.1175/1520-0477(2001)082%3C2415:FANTTS%3E2.3.CO;2

Berretta, C., Poë, S., Stovin, V. 2014. Moisture content behaviour in extensive green roofs during dry periods: The influence of vegetation and substrate characteristics. *Journal of Hydrology, 511*, 374–386. https://doi.org/10.1016/j.jhydrol.2014.01.036

Burchard-Levine, V., Nieto, H., Riaño, D., Migliavacca, M., El-Madany, T. S., Guzinski, R.,... & Martín, M. P. 2021. The effect of pixel heterogeneity for remote sensing based retrievals of evapotranspiration in a semi-arid tree-grass ecosystem. *Remote Sensing of Environment, 260*, 112440. https://doi.org/10.1016/j.rse.2021.112440

Conagua. 2023, August 31. Estadísticas agrícolas de los distritos de riego. https://www.gob.mx/conagua/documentos/estadisticas-agricolas-de-los-distritos-de-riego

Datta, S., Saleh, T., Tyson, E. O., Daniel, M., Prasanna, G., Jean, L. S. 2018. Performance Assessment of Five Different Soil Moisture Sensors under Irrigated Field Conditions in Oklahoma. *Sensors, 18*(11), 3786. https://doi.org/10.3390/s18113786

De la Fuente-Sáiz D., Ortega-Farías S., Fonseca D., Ortega-Salazar, S., Kilic, A., Allen, R. 2017. Calibration of METRIC Model to Estimate Energy Balance over a Drip-Irrigated Apple Orchard. *Remote Sensing, 9*(7), 670. https://doi.org/10.3390/rs907067.0

Feng, Y., Burian, S.J., Pardyjak, E.R. 2018. Observation and Estimation of Evapotranspiration from an Irrigated Green Roof in a Rain-Scarce Enviromen. *Water, 10*, 262. https://doi.org/10.3390/w10030262

French, A. N., Hunsaker, D. J., Thorp, K. R. 2015. Remote sensing of evapotranspiration over cotton using the TSEB and METRIC energy balance models. *Remote Sensing of Environment, 158*, 281–294. https://doi.org/10.1016/j.rse.2014.11.003

Garcia, L. A., Asce, M., Elhaddad, A., Altenhofen, J., Asce, M., Hattendorf, M. 2013. Developing Corn Regional Crop Coefficients Using a Satellite-Based Energy Balance Model (ReSET-Raster) in the South Platte River Basin of Colorado. *Journal of irrigation and drainage engineering*, *139*(10), 821–833. https://doi.org/10.1061/(ASCE)IR.1943-4774.0000616.

Gaso, D., Walter-Shea, E., Kilic, A. May 28-31, 2017. Comparison of energy balance values estimated with METRIC model with eddy covariance data for soybean and maize in rrigated and rainfed systems. *Anais do XVIII Simpósio Brasileiro do Sensoriamento Remoto-SBSR*. INPE Santos-SP, Brasil.

Gorelick, N., Hancher, M., Dixon, M., Ilyushchenko, S., Thau, D., Moore, R. 2017. Google Earth Engine: Planetary-scale geospatial analysis for everyone. *Remote Sensing of Environment, 202*, 18–27. https://doi.org/10.1016/j.rse.2017.06.031

Guillevic, P.C., J.L. Privette, B. Coudert, M.A. Palecki, J. Demarty, C. Ottlé, J.A. Augustine. 2012. Land surface temperature product validation using NOAA's surface climate observation networks: Scaling methodology for the Visible Infrared Imager Radiometer Suite (VIIRS), *Remote Sensing of Environment, 124*, 282–298. https://doi.org/10.1016/j.rse.2012.05.004

Ibarra, E.S., Bustamante, W.O., Cervantes, J.M., Pérez, C.M., Rangel, P.P. 2021. Déficit hídrico en maíz al considerar fenología, efecto en rendimiento y eficiencia en el uso del agua. *Agrociencia, 55*(3), 209-226.

Jahangir, M.H., Arast, M. 2020. Remote sensing products for predicting actual evapotranspiration and water stress footprints under different land cover. *Journal of Cleaner Production, 266*, 121818. https://doi.org/10.1016/j.jclepro.2020.121818

Jensen, M.E., Allen, R.G. 2016. Evaporation, evapotranspiration, and irrigation water requirements, Second Ed. *ASCE Manuals and Reports on Engineering Practice No. 70*, Reston, Virginia.

Kadam, S.A., Stöckle, C.O., Liu, M., Gao, Z., Russell, E.S. 2021. Suitability of earth engine evaporation flux (Eeflux) estimation of evapotranspiration in rainfed crops. *Remote Sensing, 13*(19). https://doi.org/10.3390/rs13193884

Khan, A., Stöckle, C.O., Nelson, R.L., Peters, T., Adam, J.C., Lamb, B., Chi, J., Waldo, S. 2019. Estimating biomass and yield using metric evapotranspiration and simple growth algorithms. *Agronomy Journal, 111*(2), 536–544. https://doi.org/10.2134/agronj2018.04.0248

Kilic, A., Allen, R G., Blankenau, P.A., Revelle, P., Ozturk, D., Huntington, J.L. 2020. Global production and free access to Landsat-scale Evapotranspiration with EEFlux and eeME ation with EEFlux and eeMETRIC. 6th *Decennial National Irrigation Symposium Sponsored by ASABE*, San Antonio, Texas, USA. https://doi.org/10.13031/irrig.2020-038

Kilic, A., Allen, R., Trezza, R., Ratcliffe, I., Kamble, B. 2016. Sensitivity of evapotranspiration retrievals from the METRIC processing algorithm to improved radiometric resolution of Landsat 8 thermal data and to calibration bias in Landsat 7 and 8 surface temperature. *Remote Sensing of Environment, 185, 198-209*. https://doi.org/10.1016/j.rse.2016.07.011

Laipelt, L., Henrique Bloedow Kayser, R., Santos Fleischmann, A., Ruhoff, A., Bastiaanssen, W., Erickson, T.A., Melton, F. 2021. Long-term monitoring of evapotranspiration using the SEBAL algorithm and Google Earth Engine cloud computing. *ISPRS Journal of Photogrammetry and Remote Sensing, 178*(April), 81–96. https://doi.org/10.1016/j.isprsjprs.2021.05.018

Licht, M., Archontoulis, S. 2017. Corn Water Use and Evapotranspiration. *Integrated Crop Management News*, 2441. https://crops.extension.iastate.edu/cropnews/2017/06/corn-water-use-and-evapotranspiration

Lima, J.G. A., Sánchez, J.M., Piqueras, J.G., Sobrinho, J.E., Viana, P.C., Alves, A.S. 2020. Evapotranspiration of sorghum from the energy balance by METRIC and STSEB. *Revista Brasileira de Engenharia Agrícola e Ambiental, 24*(1), 24–30. https://doi.org/10.1590/1807-1929/agriambi.v24n1p24-30

Liu, Y., Ortega-Farías, S., Fan, Y., Hou, Y., Wang, S., Yang, W., Li, S., Tian, F. 2024. Comparison of Differences in Actual Cropland Evapotranspiration under Two Irrigation Methods Using Satellite-Based Model. *Remote Sensing*, *16*(1), 175. https://doi.org/10.3390/rs16010175

Mhawej, M., Faour, G. 2020. Open-source Google Earth Engine 30-m evapotranspiration rates retrieval: The SEBALIGEE system. *Environmental Modelling and Software, 133*, 104845. https://doi.org/10.1016/j.envsoft.2020.104845

MSM. 2023. Monitor de sequía en México. CONAGUA. Consultado en https://smn.conagua.gob.mx/tools/RESOURCES/Monitor%20de%20Sequia%20en%20Mexico/MunicipiosSequia.xlsx.

Ojeda-Bustamante, W., Sifuentes-Ibarra, E., Unland-Weiss, H. 2006. Programación integral del riego en maíz en el norte de Sinaloa, México. *Agrociencia, 40*(1), 13–25. http://www.scielo.org.mx/scielo.php?script=sci_arttext&pid=S1405-31952006000100013&lng=es&tlng=es.

Ortega-Farías, S., Ortega-Salazar, S., Poblete, T., Kilic, A., Allen, R., Poblete-Echeverría, C, Ahumada-Orellana, L., Zuñiga, M, Sepúlveda, D. 2016. Estimation of Energy Balance Components over a Drip-Irrigated Olive Orchard Using Thermal and Multispectral Cameras Placed on a Helicopter-Based Unmanned Aerial Vehicle (UAV). *Remote Sensing, 8*(8), 638. https://doi.org/10.3390/rs8080638

Ortega-Salazar, S., Ortega-Farías, S., Kilic, A., Allen, R. 2021. Performance of the METRIC model for mapping energy balance components and actual evapotranspiration over a superintensive drip-irrigated olive orchard. *Agricultural Water Management, 251*, 106861. https://doi.org/10.1016/j.agwat.2021.106861.

Pereira, L.S., Allen, R.G., Smith, M., Raes. M. 2015. Crop evapotranspiration estimation with FAO56: past and future. *Agricultural Water Management, 147*, 4-20. https://doi.org/10.1016/j.agwat.2014.07.031

Pettorelli, N. (2013). *The normalized difference vegetation index*. Oxford University Press, USA. https://doi.org/10.1093/acprof:osobl/9780199693160.001.0001

Pôças, I., Paço, T.A., Cunha, M., Andrade, J.A., Silvestre, J., Sousa, A., Santos, F.L., Pereira, L.S., Allen, R.G. 2014. Satellite-based evapotranspiration of a super-intensive olive orchard: Application of METRIC algorithms. *Biosystems Engineering, 128*, 69–81. https://doi.org/10.1016/j.biosystemseng.2014.06.019

Ramírez-Cuesta, J.M., Allen, R.G., Intrigliolo, D.S., Kilic, A., Robison, C.W., Trezza, R.,... & Lorite, I.J. 2020. METRIC-GIS: An advanced energy balance model for computing crop evapotranspiration in a GIS environment. *Environmental Modelling & Software, 131*, 104770. https://doi.org/10.1016/j.envsoft.2020.104770

Ramírez-Sánchez, A.S., Ibarra-Armenta, C.I., & Leos-Rodríguez, J.A. 2021. Evaluación de la administración de la infraestructura de riego por parte de Asociaciones de Usuarios de Módulos de Riego: El caso de Culiacán 010, módulos I-3 y IV-3, 2011-2017. *Acta universitaria, 31*. https://doi.org/10.15174/au.2021.2807

Reyes-González, A., Kjaersgaard, J., Trooien, T., Hay, C., Ahiablame, L. 2017. Comparative Analysis of METRIC Model and Atmometer Methods for Estimating Actual Evapotranspiration. *International Journal of Agronomy*, https://doi.org/10.1155/2017/3632501

Reyes-González, A., Kjaersgaard, J., Trooien, T., Reta-Sánchez, D.G., Sánchez-Duarte, J.I., Preciado-Rangel, P., Fortis-Hernández, M. 2019. Comparison of leaf area index, surface temperature, and actual evapotranspiration estimated using the METRIC model and in situ measurements. *Sensors (Switzerland), 19*(8). https://doi.org/10.3390/s19081857

Rouse, J.W., Hass, R.H., Schell, J.A., Deering, D.W. 1973. Monitoring vegetation systems in the Great Plains with ERTS, *Proceedings of the Third Earth Resources Technology Satelite-1 Symposium*, Washington, D.C.: NASA. Goddart Space Flight Center, Vol. 1, pp. 309-317. (NASA SP-351).

Sharma, V., Kilic, A., Irmak, S. 2016. Impact of scale/resolution on evapotranspiration from Landsat and MODIS images, *Water Resour. Res., 52*, 1800–1819. https://doi.org/10.1002/2015WR017772

Stancalie, G., Marica, A., Toulios, L. 2010. Using earth observation data and CROPWAT model to estimate the actual crop evapotranspiration. *Physics and Chemistry of the Earth, 35*(1-2), 25-30. https://doi.org/10.1016/j.pce.2010.03.013

Suwanlertcharoen, T., Chaturabul, T., Supriyasilp, T., Pongput, K. 2023. Estimation of Actual Evapotranspiration Using Satellite-Based Surface Energy Balance Derived from Landsat Imagery in Northern Thailand. *Water, 15*, 450. https://doi.org/https://doi.org/10.3390/w15030450

Tasumi, M. 2003. *Progress in operational estimation of regional evapotranspiration using satellite imagery*. PhD Thesis, University of Idaho. Moscow, ID, USA.

Tasumi, M. 2019. Estimating evapotranspiration using METRIC model and Landsat data for better understandings of regional hydrology in the estern Urmia Lake Basin. *Agriculture Water Management, 226*, 105805. https://doi.org/10.1016/j.agwat.2019.105805

Verma, B., Prasad, R., Srivastava, P.K., Yadav, S.A., Singh, P., & Singh, R.K. 2022. Investigation of optimal vegetation indices for retrieval of leaf chlorophyll and leaf area index using enhanced learning algorithms. *Computers and electronics in agriculture, 192*, 106581. https://doi.org/10.1016/j.compag.2021.106581

Volk, J.M., Huntington, J.L., Melton, F.S. *et al.* 2024. Assessing the accuracy of OpenET satellite-based evapotranspiration data to support water resource and land management applications. *Nature Water, 2*, 193–205. https://doi.org/10.1038/s44221-023-00181-7

Xue, J., Bali, K.M., Light, S., Hessels, T., Kisekka, I. 2020. Evaluation of remote sensing-based evapotranspiration models against surface renewal in almonds, tomatoes and maize. *Agricultural Water Management, 238*, 106228. https://doi.org/10.1016/j.agwat.2020.106228

Zawilski, B.M., Granouillac, F., Claverie, N., Lemaire, B., Brut, A., Tallec, T. 2023. Calculation of soil water content using dielectric-permittivity-based sensors – benefits of soil-specific calibration, *Geoscientific Instrumentation, Methods and Data Systems, 12*, 45–56, https://doi.org/10.5194/gi-12-45-2023.